Aspirin-Trigge red-Resolvin D1 reduces mucosal inflammation and promotes resolution in a murine model of acute lung injury

Published in final edited form as:
Mucosal Immunol. 2013 March ; 6(2): 256–266. doi:10.1038/mi.2012.66.

Aspirin-Trigge red-Resolvin D1 reduces mucosal inflammation and promotes resolution in a murine model of acute lung injury

O. Eickmeier[1], **H. Seki**[1], **O. Haworth**[1], **JN. Hilberath**[1], **F. Gao**[2], **M. Uddin**[1], **RH. Croze**[1], **T. Carlo**[1], **MA. Pfeffer**[1], and **BD. Levy**[1,2,*]

[1]Pulmonary and Critical Care Medicine, Department of Internal Medicine, Brigham and Women's Hospital and Harvard Medical School, Boston, Massachusetts, USA

[2]Center for Experimental Therapeutics and Reperfusion Injury, Department of Anesthesiology, Perioperative and Pain Medicine, Brigham and Women's Hospital and Harvard Medical School, Boston, Massachusetts, USA

Abstract

Acute Lung Injury (ALI) is a severe illness with excess mortality and no specific therapy. Protective actions were recently uncovered for docosahexaenoic acid -derived mediators, including D-series resolvins. Here, we used a murine self-limited model of hydrochloric acid-induced ALI to determine the effects of aspirin-triggered resolvin D1 (AT-RvD1) on mucosal injury. RvD1 and its receptor ALX/FPR2 were identified in murine lung after ALI. AT-RvD1 (~0.5 – 5 μg/kg) decreased peak inflammation, including bronchoalveolar lavage fluid (BALF) neutrophils by ~75%. Animals treated with AT-RvD1 had improved epithelial and endothelial barrier integrity and decreased airway resistance concomitant with increased BALF epinephrine levels. AT-RvD1 inhibited neutrophil-platelet heterotypic interactions by down-regulating both P-selectin and its ligand CD24. AT-RvD1 also significantly decreased levels of BALF pro-inflammatory cytokines, including IL-1β, IL-6, KC and TNF-α, and decreased NF-κB phosphorylated p65 nuclear translocation. Together, these findings indicate that AT-RvD1 displays potent mucosal protection and promotes catabasis after ALI.

INTRODUCTION

Acute lung injury (ALI) and the acute respiratory distress syndrome (ARDS) are life-threatening disorders that contribute significantly to critical illness[1]. Approximately 75,000 patients die from ARDS each year in the United States[2]. Respiratory failure from ALI or ARDS is a frequent cause of admission to intensive care units, often requiring ventilatory support. Despite advances in understanding ARDS pathophysiology, no medical interventions have proven effective in improving the outcome of patients with ALI/ARDS[3, 4]. Aspiration pneumonitis is one of the leading causes of ALI/ARDS that in most instances is self-limited[5], suggesting the existence of endogenous, host protective mechanisms.

While the cellular events that return the injured lung to homeostasis have been described by histopathology, there remains only a limited understanding of the molecular mechanisms

*Corresponding author: Bruce D. Levy, MD, Pulmonary and Critical Care Medicine, Department of Internal Medicine, Brigham and Women's Hospital and Harvard Medical School, Harvard Institutes of Medicine Bldg, 77 Avenue Louis Pasteur (HIM 855), Boston, MA 02115, USA, Phone: 617-525-5407, Fax: 617-525-5413, blevy@partners.org.

DISCLOSURES

BDL is an inventor on patents assigned to Brigham and Women's Hospital and Partners HealthCare on the uses of anti-inflammatory and pro-resolving lipid mediators. These are licensed for clinical development.

underlying this catabatic process. Polyunsaturated fatty acids (PUFAs) appear to play important roles in ALI and its resolution. Activation of pulmonary leukocytes leads to increased generation of arachidonic acid-derived eicosanoids that can serve as important mediators of inflammation, vascular leak, and tissue catabasis[6–8]. In contrast, omega-3 fatty acid-based nutritional supplementation can significantly improve oxygenation and decrease the length of stay in an intensive care unit, time on mechanical ventilation, occurrence of new organ failure, and mortality[9–11].

Airway mucosa is enriched with the omega-3 fatty acid docosahexaenoic acid (DHA)[12]. Resolvin D1 (RvD1) is a DHA-derived mediator first identified in resolving peritoneal exudates[13]. Aspirin acetylates cyclooxygenase-2 (COX-2) to lead to the formation of aspirin-triggered mediators, including the 17R-epimer of RvD1 termed aspirin-triggered RvD1 (AT-RvD1)[13, 14] that decreases leukocytic infiltration in murine peritonitis to a greater extent than RvD1 and is more resistant to catalysis than RvD1[14]. Of interest, both COX-2 and aspirin may have beneficial actions in ALI/ARDS[15, 16]. Here, in a non-lethal model of ALI, AT-RvD1 decreased lung inflammation after mucosal injury and promoted ALI resolution by enhancing restitution of barrier integrity, decreasing circulating neutrophil-platelet heterotypic interactions, and regulating inflammatory mediators and NF-κB activation.

RESULTS

RvD1 and 17-HDHA are generated after mucosal injury

To determine if endogenous DHA is converted to RvD1 after ALI, murine lungs were obtained 12h after ALI from intratracheal HCl (0.1 N, pH 1.5) and lipids were extracted from lung homogenates for analyses (see Methods). Both RvD1 and its biosynthetic precursor 17(S)-hydroxy-DHA (17-HDHA) were identified by LC-MS/MS based metabololipidomics analysis (Fig. 1a–c). At this time point, RvD1 was present in pg quantities.

ALX/FPR2 receptors are expressed on lung epithelial cells and macrophages

RvD1 and AT-RvD1 are anti-inflammatory and pro-resolving agonists at ALX/FPR2 receptors[17,18], so expression of ALX/FPR2 was determined by immunohistochemistry in murine lung at baseline and after ALI (Fig. 1d–g). ALX/FPR2 receptors were expressed at low levels in uninjured lungs, in particular in airway epithelial cells and alveolar macrophages (Fig. 1d–e). As early as two hours after ALI, there was an evident increase in mucosal epithelial cell ALX/FPR2 expression (Fig. 1f) that was further increased 12h after ALI (Fig. 1g).

AT-RvD1 reduces leukocyte recruitment after airway mucosal injury

With both RvD1 and its receptor ALX/FPR2 present in murine lung, we determined the impact of exogenous AT-RvD1 on inflammatory responses after ALI. Because RvD1 is rapidly inactivated [14], its epimer AT-RvD1, which partially resists metabolic inactivation, was chosen for study. Like RvD1, AT-RvD1 is an agonist at ALX/FPR2 receptors [18]. In a first series of experiments, AT-RvD1 or a vehicle control (0.1% ethanol (vol/vol)) were administered intravenously 15 minutes prior to instillation of HCl (0.1 N, pH 1.5) into the left mainstem bronchus (Fig. 2a). AT-RvD1 led to significant and dose dependent decrements in total BALF cell numbers 12 hours after ALI (67,500 ± 15,880 total BALF cells (AT-RvD1 10ng, n=5); 53,810 ± 7836 total BALF cells (AT-RvD1 100ng, n=10); mean ± SEM) relative to vehicle control mice (129,800 ± 10,230 total BALF cells; mean ± SEM; n=12, $p<0.01$) (Fig. 2b). In particular, AT-RvD1 decreased BALF neutrophils (PMNs) (11,550 ± 4,841 PMNs (AT-RvD1 10ng, n=5); 8,258 ± 2,988 PMNs (AT-RvD1

100ng, n=10); mean ± SEM) relative to vehicle (36,650 ± 5,649 PMNs (n=12); mean ± SEM, $p<0.01$) (Fig 2c). BALF macrophages (MACs) were also decreased with AT-RvD1 (44,470 ± 7,846 MACs; (AT-RvD1 100ng, n=10); mean ± SEM) in comparison to vehicle (91,130 ± 10,890 MACs; mean ± SEM, n = 12, $p<0.01$) (Fig. 2d).

In a second series of experiments to determine its pro-resolving and potential therapeutic properties, AT-RvD1 was given two hours after airway injury (Fig. 2e). When administered post-injury, AT-RvD1 also mediated significant decreases in total BALF cells (87,860 ± 14,550 (100ng, n=7); 130,000 ± 7,935 (vehicle, n=6); mean ± SEM, $p<0.05$) (Fig. 2f) and BALF PMNs (10,520 ± 1,404 (100ng, n=7); 33,410 ± 4,885 (vehicle, n=6); mean ± SEM, $p<0.01$) (Fig. 2g). No significant changes of the numbers of BALF MACs were present when AT-RVD1 (100ng) was given after injury (Fig. 2h).

In a third series of experiments to investigate AT-RvD1's impact on early leukocyte trafficking after ALI, airway inflammation was monitored by BAL two hours and six hours after ALI. While no significant differences in the numbers of total BALF cells were identified between AT-RvD1 dosing before (−15 min) or after (+2hr) ALI, there was a lower amplitude and earlier decrease in airway inflammation in mice that received AT-RvD1 prior to ALI. These changes in early BALF cell numbers were correlated with BALF MACs, as significant numbers of BALF PMNs were not evident until twelve hours after ALI (Fig. 2i–k).

AT-RvD1 decreases lung edema and neutrophil accumulation after ALI

ALI from HCl instillation led to increased alveolar edema and inflammation (PMNs identified as Ly-6G$^+$ by immunostaining) (Fig. 3a). Administration of AT-RvD1 (100 ng) either before (Fig. 3b) or 2 hours after (Fig. 3c) intratracheal acid instillation decreased both alveolar edema and the numbers of Ly-6G$^+$ cells relative to control mice receiving only vehicle.

Regulation of lung neutrophil recruitment by AT-RvD1

To investigate the PMN recruitment pattern with AT-RvD1, its influence on intravascular and interstitial PMNs was determined (see Methods). Just prior to harvesting murine lungs 12 hours after ALI, a PMN specific Gr-1 antibody was injected intravenously to label intravascular PMNs. After BAL, the lungs were collected, prepared for FACS and stained with a second PMN specific antibody (NIMP-14R) (see Methods). PMNs were identified by forward/side scatter profiles and cells that were Gr-1$^+$NIMP-14R$^+$ were consistent with intravascular PMNs and cells that were Gr-1$^-$NIMP-14R$^+$ were consistent with interstitial PMNs (Fig. 4a). The percent interstitial and intravascular PMNs at this time point were decreased only slightly with AT-RvD1 (100 ng) relative to vehicle control, and these differences did not reach statistical significance (Fig. 4b–c). Of interest, the number of circulating PMNs (1,255 ± 108 PMNs/μl, mean ± SEM) and monocytes (468 ± 37 Monos/μl, mean ± SEM) were markedly increased twelve hours after ALI relative to control animals without injury (243 ± 56 PMNs/μl; 153 ± 57 Monos/μl) (n=5, $p<0.05$) (Fig. 4d–g). Intravenous AT-RvD1 significantly decreased the numbers of PMNs (866 ± 59 PMNs/μl, mean ± SEM) and Monos (240 ± 63 Monos/μl, mean ± SEM) in the peripheral blood of acid-injured mice (n=5, $p<0.05$) (Fig. 4d–g).

AT-RvD1 reduces lung resistance in ALI

To investigate whether treatment with AT-RvD1 had a measurable effect on lung mechanics, we determined lung function in mechanically-ventilated, anesthetized mice. Because of the unilateral and mild nature of the ALI in this model, marked changes in tissue elastance are not observed[8] and no significant differences were evident with AT-RvD1

relative to vehicle controls (Fig. 5a). Of interest, the increased lung resistance 12h after ALI in this model was significantly reduced by AT-RvD1 (100ng) given either before (0.65 ± 0.05 cmH_2O*s/ml, mean ± SEM, n= 12) or after ALI (0.56 ± 0.02 cmH_2O*s/ml, mean ± SEM, n= 6) in comparison to vehicle (0.90±0.08 cmH_2O*s/ml, mean ± SEM, n= 10, p< 0.05) (Fig. 5b).

AT-RvD1 enhances restitution of barrier function after ALI

Because leakage permeability changes are integral to acute inflammation and ALI and lung histology revealed that AT-RvD1 decreased alveolar edema (Fig. 3), the actions of AT-RvD1 on both epithelial and endothelial barrier integrity were next determined. To measure the effects of AT-RvD1 on the restitution of epithelial barrier function after direct mucosal injury by HCl, fluorescently labeled dextran was instilled intratracheally and 10 minutes later BALF and right ventricular blood were obtained for measurement of fluorescence (see Methods). The ratio of fluorescence in serum to BALF provided an index of epithelial permeability. 12 hours after acid instillation, epithelial permeability is increased and control mice receiving only vehicle gave serum/BALF fluorescence ratio of 0.36 ± 0.07 (mean ± SEM, n=5) (Fig. 5c). AT-RvD1 (100ng) significantly improved epithelial barrier disruption 12h after mucosal injury with decreased serum/BALF fluorescence ratios relative to vehicle controls when the compound was given either before injury (0.08 ± 0.03, mean ± SEM, n=3, p < 0.05) or two hours after injury (0.09 ± 0.02, mean ± SEM, n=5, p<0.01) (Fig. 5c). Direct actions for the compound on epithelial barrier integrity *in vitro* were not identified, as AT-RvD1 (1–100nM) did not significantly change the trans-epithelial electrical resistance of Calu-3 human bronchial epithelial cells in culture. AT-RvD1 improved vascular permeability changes *in vivo*, as the amount of Evans Blue dye that extravasated into BALF was significantly decreased in mice receiving AT-RvD1 (100ng) either before injury (4.7 ± 0.2 μg/ml, mean ± SEM, n=3, p<0.01) or two hours after injury (4.6 ± 0.8 μg/ml, mean ± SEM, n = 3, p<0.05) in comparison to vehicle control mice (8.5± 0.8 μg/ml, n=4) (Fig. 5d).

AT-RvD1 decreases neutrophil-platelet interactions

Vascular inflammation with heterotypic interactions between PMNs, platelets and endothelial cells are important early events in ALI[19,20]. To determine if AT-RvD1 regulated these cell-cell interactions, blood was obtained from mice given either AT-RvD1 (100ng) or vehicle alone and analyzed by flow cytometry (Fig. 5e). PMNs were identified by their physical properties and Ly-6G staining. PMN-platelet interactions were identified as PMNs ($Ly\text{-}6G^+$) that were also $CD41^+$ (platelets), and AT-RvD1 decreased the percent $Ly\text{-}6G^+CD41^+$ cells. P-selectin (CD62P) plays important roles in PMN-platelet interactions in ALI[19,20] and AT-RvD1 decreased the numbers of $Ly\text{-}6G^+CD62P^+$ cells (Fig. 5e). Western blot analysis of lung tissue homogenates also revealed decreased expression of both CD62P and its granulocyte receptor CD24 in mice receiving AT-RvD1 (Fig. 5f).

Endogenous airway epinephrine levels are enhanced by AT-RvD1

Because AT-RvD1 decreased lung resistance after ALI (Fig. 5b), BALF epinephrine levels were next determined using a specific and sensitive ELISA (see Methods). BALF epinephrine levels were significantly increased in mice that had received AT-RvD1 (100ng) either before injury (201.4 ± 13.2 pg/mL, mean ± SEM) or after injury (310 ± 37.1 pg/mL, mean ± SEM) in comparison to vehicle (146.7 ± 8.4 pg/mL, mean ± SEM, n ≥ 6, p< 0.01) (Fig. 6a).

AT-RvD1 decreases pro-inflammatory mediator release after ALI

To determine the impact of AT-RvD1 on inflammatory mediators after ALI, BALF levels of select cytokines, chemokines and lipid mediators were determined. BALF TGF-β was

significantly increased when AT-RvD1 was administered two hours after ALI (Fig. 6b). BALF levels of the counter-regulatory mediators lipoxin A_4 (LXA_4) and IL-10 did not increase with AT-RvD1 relative to vehicle; however, the LXA_4 and IL-10 levels were significantly different between the two AT-RvD1 treatment strategies (Fig. 6c–d). When AT-RvD1 was given before HCl, LXA_4 and IL-10 levels decreased, but there was no significant change in LXA_4 and IL-10 levels when AT-RvD1 was given two hours after injury (Fig. 6c–d). Several pro-inflammatory mediators were significantly decreased in AT-RvD1 treated mice, including IL-1β, IL-6, KC and TNF-α (Fig. 6e–h). No significant changes were observed in BALF CCL3, CXCL2, CXCL10 and LTB_4 (Fig. 6i–l). In addition, levels of 8-isoprostane, a sensitive marker of oxidative stress, are low at this time point in this model [8], and there were no significant changes apparent with AT-RvD1 (data not shown).

AT-RvD1 decreases NF-κB p65 translocation after ALI

Because AT-RvD1 markedly decreased several pro-inflammatory cytokines, the impact of AT-RvD1 on NF-κB activation and the cellular targets for AT-RvD1 counter-regulatory actions were next determined by immunohistochemistry of lung sections. NF-κB activation and nuclear translocation was identified using a phosphorylated p65 (serine 276) antibody (see Methods). There was an increase in NF-κB phosphoserine p65 abundance and nuclear translocation in airway epithelial cells and lung macrophages that was evident two hours after ALI (Fig. 7a–c) and markedly increased twelve hours after ALI (Fig. 7d). Both dosing strategies for AT-RvD1 decreased the abundance of NF-κB phosphoserine p65 in epithelial cells and macrophages twelve hours after HCl (Fig. 7e–f).

DISCUSSION

Alveolar edema and PMN recruitment and activation are early events in acute mucosal inflammation and ALI/ARDS[1]. These cellular events are subject to regulation by lipid mediators[6,19], and here RvD1 was generated after HCl-initiated ALI. The RvD1 receptor ALX/FPR2 is expressed on PMNs, monocytes, macrophages and airway epithelial cells[21,22,17,23]. Murine ALX/FPR2 lung expression was evident in airway epithelial cells and macrophages and its abundance markedly increased after ALI. The RvD1 epimer AT-RvD1 displayed properties of both an anti-inflammatory and pro-resolving mediator in decreasing the severity of HCl acid-initiated ALI. Given either before or shortly after mucosal injury, AT-RvD1 reduced several parameters of alveolar edema 12 hours after ALI, including by histological evidence, and measures of epithelial and endothelial permeability. There was an increase in lung tissue resistance after intratracheal administration of HCl that was reduced by AT-RvD1 and associated with AT-RvD1-mediated increases in endogenous BALF epinephrine levels. In addition to these actions on mucosal tissue resident cells, AT-RvD1 also displayed potent leukocyte-directed actions, including decreased circulating PMNs and monocytes, vascular PMN-platelet heterotypic interactions, airway PMN infiltration, BALF pro-inflammatory mediator levels and NF-κB p65 activation in airway epithelial cells and macrophages. Together, these findings indicate that in lung tissue and inflammatory cells AT-RvD1 harnessed several cell-type specific protective mechanisms to decrease ALI severity. AT-RvD1's regulation of vascular PMN-platelet interactions, permeability changes and epinephrine levels emphasize the importance of vascular inflammatory events in the pathogenesis of early ALI.

Retrospective analyses of patients with ARDS have identified aspirin as a protective exposure that decreases ARDS morbidity and mortality[16]. In addition to inhibiting platelet function, aspirin triggers the formation of specific pro-resolving mediators[24], including AT-RvD1 from DHA in inflamed murine and human tissues[14]. In murine models of acute inflammation, AT-RvD1 decreases production of pro-inflammatory mediators and regulates

leukocyte trafficking to inflammatory sites (reviewed in reference 25), including in experimental models of arthritis and colitis[26,27]. Here, AT-RvD1 decreased lung PMN infiltration and decreased inflammatory responses by tissue resident cells, including endothelial and epithelial barrier function and levels of several pro-inflammatory mediators in the injured lung. AT-RvD1 two hours after injury gave similar protection as a dose given 15 minutes prior to injury, indicating that AT-RvD1 could accelerate the resolution of ALI.

Neutrophil activation can cause bystander tissue damage that contributes to the pathogenesis of ALI/ARDS[28], so decreasing lung PMN accumulation and pro-inflammatory mediators would be predicted to have synergistic benefit for tissue protection and catabasis after acid injury. To this end, inhibition of PMN function in animal studies attenuates lung injury induced by models of gastric acid aspiration[29,30]. RvD1 transduces potent anti-inflammatory actions for PMNs. Single cell PMN assays in microfluidic chambers have uncovered direct PMN actions for RvD1, but not the parent fatty acid DHA, to rapidly stop PMN migration towards the chemoattractant IL-8[31] and RvD1 can regulate PMN lung recruitment in response to LPS[32]. Here, early administration of AT-RvD1 appeared to reduce the amplitude and duration of acid-initiated ALI and together with AT-RvD1's regulation of NF-κB activation suggests that the compound's reduction in airway inflammation is secondary to both direct actions on leukocytes and indirect actions to decrease the levels of inflammatory cytokines. In addition, AT-RvD1's actions on leukocytes to decrease their lung recruitment in conjunction with regulation of vasoactive mediators likely accounts for the decrease in alveolar edema with AT-RvD1. In this regard, at ocular mucosal surfaces, RvD1 decreases cysteinyl leukotrienes[33] that also play a pivotal role in vascular permeability in HCl-induced ALI[8].

Lipoxins (LXs) are arachidonic acid-derived mediators that display anti-inflammatory and pro-resolving actions, including inhibition of *in vivo* PMN activation, cytokine release, and angiogenesis (reviewed in reference 25). These protective actions are mediated, in part, by the lipoxin A_4 receptor ALX/FPR2 that can also serve as an anti-inflammatory receptor for RvD1 and AT-RvD1[17,18,23]. ALX/FPR2 receptor expression is increased *in vitro* after airway epithelial injury[21] and transgenic expression of human ALX/FPR2 receptors is protective from HCl-initiated ALI[15]. Here, ALX/FPR2 receptor expression increased *in vivo* 12 hours after ALI in both airway epithelial cells and lung macrophages, and AT-RvD1 administration markedly decreased NF-κB activation in these ALX/FPR2 expressing cells. While apoptotic PMNs are difficult to identify in this model of ALI, RvD1 in other model systems are potent stimuli for macrophage efferocytosis during tissue catabasis[17] and can promote host catabatic responses that in conjunction with antibiotics promotes the resolution of bacterial infection[34]. Of interest, BALF levels of LXA_4 were significantly decreased by AT-RvD1 administration before injury, which were significantly lower than LXA_4 levels in mice that received AT-RvD1 after injury. There are two implications of this finding. First, AT-RvD1's protective actions are independent of LXA_4 generation and second, the early events in host acute inflammatory responses to tissue injury are critical to endogenous biosynthesis of LXA_4. Early pro-inflammatory mediator formation is pivotal to lipid mediator class-switching for the later generation of anti-inflammatory mediators, such as LXA_4[35,15]. Administration of AT-RvD1 before injury dampened the early pro-inflammatory mediator production with reductions in endogenous LXA_4 generation 12 hours later. Because AT-RvD1 resists rapid inactivation[14] and promoted ALI resolution, the decrements in LXA_4 generation did not have adverse consequences on lung catabasis. This is in sharp contrast with chemical inhibitors of early inflammatory mediator generation, such as COX-2 specific inhibitors or 5-lipoxygenase inhibition, which can be resolution "toxic" for tissue injury or inflammation[15,36].

P-selectin (CD62P) is expressed by activated endothelial cells and platelets as a molecular regulator of heterotypic PMN-platelet and platelet-endothelial cell interactions[37]. During secondary capture, PMNs interact with circulating or endothelial adherent platelets to augment PMN-endothelial interactions in inflamed vascular beds for PMN tissue recruitment[38] Of note, platelet depletion leads to diminished leukocyte recruitment in tissue inflammation and ALI[19]. As a measure of vascular inflammation, heterotypic cell-cell interactions between PMNs and platelets were monitored here in blood from the right ventricle, just prior to entering the pulmonary vasculature. The peripheral blood leukocytosis induced by ALI was decreased by AT-RvD1 and flow cytometry revealed a substantial reduction in PMN-platelet interactions with AT-RvD1. In addition, the expression of P-selectin (CD62P) and its PMN ligand CD24 was decreased by AT-RvD1 in lung homogenates after ALI. Blocking P-selectin–dependent platelet-PMN interactions is highly protective in a similar model of acid-initiated ALI[19]. In addition to circulating PMNs and platelet-PMN interactions, resolvins can also decrease ADP-stimulated platelet aggregation[39]. These findings suggest that AT-RvD1's mucosal protection in ALI resulted, in part, from its actions on PMNs that decreased PMN recruitment from bone marrow to lung and decreased PMN-mediated disruption of lung barrier integrity by regulating PMN interactions in the vasculature with platelets. Together, these findings indicate the presence of unique homeostatic pathways for DHA-derived bioactive mediators inthe lung.

AT-RvD1 is a potent regulator of mucosal inflammation and can promote an array of protective responses for lung catabasis after ALI. In addition, it is notable that the pharmacologically active dose of AT-RvD1 administered i.v. was less than 100ng per mouse, or ~0.005 mg/kg, providing evidence of this compound's potent anti-inflammatory and pro-resolving actions. Enteric feeding with DHA can markedly reduce ALI/ARDS morbidity and mortality, in part via marked decreases in lung PMNs and inflammatory mediators[9,10]. The potential for lung protection by DHA-derived mediators is also supported by evidence from *fat-1* transgenic mice that are protected from ALI[40] and allergic airway inflammation[41]. These transgenic mice express the *Caenorhabditis elegans* ω-3 desaturase fat-1 gene and can endogenously generate ω-3 PUFAs from ω-6 PUFAs[39] and resolvins[41]. Moreover, AT-RvD1's epimer RvD1 displays protective actions in an LPS model of acute lung inflammation and injury[32].

In summary, our findings have uncovered new roles for AT-RvD1 in promoting resolution of acid-initiated experimental ALI. In this study, the DHA-derived lipid mediator AT-RvD1 decreased acid-initiated ALI by direct actions on circulating leukocytes and platelets with lung protective effects on barrier function, PMN accumulation and pro-inflammatory mediator generation. Expression of ALX/FPR2 receptors and AT-RvD1's regulation of NF-κB in lung mucosal epithelial cells and macrophages suggest important roles for these cells in lung tissue catabasis that will serve as a focus of future studies. Together, these results suggest a potential new therapeutic approach to the important clinical problem of ALI/ARDS that emphasizes natural resolution signaling pathways.

METHODS

Acid-initiated acute lung injury (ALI) and treatment with AT-RVD1

All mice were maintained under specific pathogen-free conditions. All studies were reviewed and approved by the Harvard Medical Area standing committee on animals (protocol # 03618). As in reference 15, hydrochloric acid (0.1 N HCl, pH 1.5, 50μl, endotoxin free; Sigma-Aldrich) was instilled selectively into the left mainstem bronchus of anesthetized mice (FVB, male, 10–12 wk; CharlesRiver) via a 24-gauge angiocatheter inserted intratracheally. Some mice received AT-RvD1 (7S,8R,17R-trihydroxy-4Z,9E,11E, 13Z,15E,19Z-docosa-hexaenoic acid; 10ng or 100ng) or vehicle (0.1% (vol/vol) ethanol) in

saline by intravenous injection either 15 minutes before ALI or 2 hours after ALI was initiated. At select time points (2, 6 and 12 hours) after acid instillation, bilateral bronchoalveolar lavage (BAL) was performed with 2 aliquots of 1ml of PBS plus 0.6mM EDTA.

Leukocyte recruitment after ALI

The total cell counts and leukocyte differential in BAL fluids (BALFs) were determinedas previously described[8]. Briefly, total cells in BALFs were counted using a hemocytometer, and a leukocyte differential count was performed after Wright-Giemsa staining.

To determine intravascular and interstitial PMNs, FITC-Gr-1 (Clone RB6-8C5, eBioscience, San Diego, CA) was intravenously injected 5 minutes prior to lung harvest (similar to 19). After BAL, the lungs were removed, dispersed and passed through a 70-μm cell strainer (as in 42). PMNs were identified during flow cytometry by their forward/side scatter profiles and their expression of NIMP-14R (Santa Cruz Biotechnology, Santa Cruz, CA) and Gr-1. Isotype control antibodies were used for compensation for nonspecific binding. The FITC-Gr-1 Ab was used to identify PMNs in the intravascular ($NIMP\text{-}14R^{+}Gr\text{-}1^{+}$) and interstitial ($NIMP\text{-}14R^{+}Gr\text{-}1^{-}$) compartments. Flow cytometry was performed using a BD FACS Canto II flow cytometer (Becton Dickinson, San Jose, CA) and data were analyzed using FlowJo software (Tree Star, Ashland, OR).

Complete blood count and differential count

Murine blood was drawn from the inferior vena cava and lysed with RBC lysis buffer (eBioscience). Leukocytes were counted with a hemocytometer and differential count was performed after Wright-Giemsa staining. For the leukocyte differential, a minimum of 200 cells were counted per slide.

Neutrophil-platelet interactions

Whole blood was collected from mice that received either AT-RvD1 (100ng) or vehicle 2 hours after ALI. Blood was lysed using 10 volumes of red blood cell lysis buffer (eBioscience) per manufacturer's instructions. For flow cytometry, cells were blocked with CD16/32 Fc block (eBioscience) and then stained with Ly6G (eBioscience), CD41 (eBioscience) or CD62P (eBioscience) for 20 minutes on ice. CD24 and P-selectin protein abundance in lung homogenates was determined by Western blot analyses. β-actin was used as a control. Antibodies were used in the manufacturer's recommended concentrations (1 μg/ml) (Santa Cruz Biotechnology).

Identification of RvD1 in murine lung

FVB mouse lungs were suspended in 1.0 mL cold methanol and gently ground followed by protein precipitation for 12 hr. Samples were next extracted by SPE column and methyl formate fractions were taken for LC-MS/MS-based lipidomics. LC-MS/MS was performed with an Agilent 1100 HPLC (Agilent Technologies, Santa Clara, CA) equipped with an Agilent Eclipse Plus C-18 column (4.6 mm×50 mm×1.8 μm) paired with an ABI Sciex Instruments 5500 QRAP linear ion trap triple quadrupole mass spectrometer (Applied Biosystems, Foster City, CA). Instrument control and data acquisition were performed using AnalystTM 1.5 software (Applied Biosystems). The mobile phase consisted of methanol/water/acetic acid (55/45/0.01; v/v/v) and was ramped to 88/12/0.01 (v/v/v) after 10 min, 100/0/0.01 (v/v/v) after 18 min, and 55:45:0.01 (v/v/v) after 1 minute to wash and equilibrate the column. Mass spectrometry analyses were carried out in negative ion mode using multiple reaction monitoring (MRM) of established specific transitions for 17-HDHA (m/z 343>245) and RvD1 (m/z 375>215). Identification was matching retention time and

diagnostic ions to synthetic standards[43]. Quantification was performed using standard calibration curves for each, and recoveries were calculated using deuterated internal standard (d_4-PGE_2)

Histology and Immunohistochemistry

After dissection, lungs were perfusion-fixed at 20 cmH_20 in IHC zinc fixative buffer (BD Pharmingen, San Diego, CA). Tissue blocks were obtained from midsagittal slices of lungsembedded in paraffin for staining with hematoxylin and eosin (Sigma). For Ly-6G (1/100 dilution, BD Pharmingen) immunostaining, tissue sections were de-paraffinized and incubated for 1 hour at room temperature with anti-mouse Ly-6G antibody to stain for PMNs. For ALX/FPR2 (1/50 dilution, Santa Cruz Biotechnology) and phosphorylated p65 subunit of NF-κB (phospho S276, 1/50 dilution, Abcam) immunostaining, tissue sections were incubated overnight at 4°C.

Determination of Barrier Integrity

FITC-Dextran was utilized as a marker of epithelial barrier disruption (as in reference 42 with minor modification). Briefly, FITC-Dextran (50mg/kg mouse) was given intratracheally via a 24-gauge angiocatheter. BAL with 1ml PBS was performed 10 minutes later with concurrent collection of blood from the right ventricle. BAL and serum were loaded onto a microwell plate and fluorescence was determined (excitation, 490nm; emission, 520nm). The ratio of serum to BALF fluorescence was used as an index of airway epithelial permeability. To measure vascular permeability, Evans Blue dye was utilized as a marker for endothelial barrier disruption (as in 8). Briefly, Evans Blue dye (40 mg/kg) was injected via tail vein and 30 minutes later BAL was performed with 1ml PBS. Extravasation of dye into BALFs was quantified by spectrophotometry (absorbance at 650nm).

Measurement of Lung Mechanics

For measurement of tissue elastance and lung resistance, mice were anesthetized with pentobarbital (70 mg/kg, i.p.; Abbott Laboratories, North Chicago, IL, USA) and mechanically ventilated with a flexiVent small animal ventilator (SCIREQ, Montreal, Canada). Lung mechanics were determined in anesthetized, ventilated animals.

Mediator levels in BALFs

Select cytokines, chemokines and total TGF beta 1 were measured in aliquots of BALF by cytokine bead array (Aushon Biosystems, Billerica, MA). BALF epinephrine, LTB_4, 8-IP, IL-10 and LXA_4 levels were measured with specific ELISAs per manufacturer's instructions (Rocky Mountain Diagnostics, Colorado Springs, CO (epinephrine); Cayman Chemical, Ann Arbor, MI (LTB_4, 8-IP); eBioscience, San Diego, CA (IL-10); Neogen, Lexington, KY (LXA_4)).

Statistical analysis

Data are expressed as the mean value ± SEM unless otherwise indicated. Analysis of variance was used to determine significance for differences between more than 2 groups. For analyses between 2 groups, cohorts were compared by Mann-Whitney-U-test. Significance was determined with P values ≤ 0.05. Statistics were performed using GraphPad Prism 5 for Windows (San Diego, CA).

Acknowledgments

We thank GuangLi Zhu and Bonna Ith for technical assistance. This research was supported in part by the US National Institutes of Health grants HL068669, AI068084 and P01-GM095467 and postdoctoral fellowships from

the American Lung Association and German Society of Pediatric Pulmonology. The content is solely the responsibility of the authors and does not necessarily reflect the official views of NHLBI, NIAID, NIGMS or the National Institutes of Health.

References

1. Ware LB, Matthay MA. The acute respiratory distress syndrome. N Engl J Med. 2000; 342:1334–1349. [PubMed: 10793167]
2. Rubenfeld GD, et al. Incidence and outcomes of acute lung injury. N Engl J Med. 2005; 353:1685–1693. [PubMed: 16236739]
3. Bernard GR, et al. The American-European Consensus Conference on ARDS. Definitions, mechanisms, relevant outcomes, and clinical trial coordination. Am J Respir Crit Care Med. 1994; 149:818–824. [PubMed: 7509706]
4. Wheeler AP, Bernard GR. Acute lung injury and the acute respiratory distress syndrome: a clinical review. Lancet. 2007; 369:1553–1564. [PubMed: 17482987]
5. Marik PE. Aspiration pneumonitis and aspiration pneumonia. N Engl J Med. 2001; 344:665–671. [PubMed: 11228282]
6. Serhan CN. Preventing injury from within, using selective cPLA2 inhibitors. Nat Immunol. 2000; 1:13–15. [PubMed: 10881166]
7. Serhan CN. Resolution phase of inflammation: novel endogenous anti-inflammatory and proresolving lipid mediators and pathways. Annu Rev Immunol. 2007; 25:101–137. [PubMed: 17090225]
8. Hilberath JN, et al. Resolution of Toll-like receptor 4-mediated acute lung injury is linked to eicosanoids and suppressor of cytokine signaling 3. FASEB Journal. 2011; 25:1827–1835. [PubMed: 21321188]
9. Gadek JE, et al. Effect of enteral feeding with eicosapentaenoic acid, gamma-linolenic acid, and antioxidants in patients with acute respiratory distress syndrome. Enteral Nutrition in ARDS Study Group.[comment]. Critical Care Medicine. 1999; 27:1409–1420. [PubMed: 10470743]
10. Pacht ER, et al. Enteral nutrition with eicosapentaenoic acid, gamma-linolenic acid, and antioxidants reduces alveolar inflammatory mediators and protein influx in patients with acute respiratory distress syndrome. Critical Care Medicine. 2003; 31:491–500. [PubMed: 12576957]
11. Singer P, et al. Benefit of an enteral diet enriched with eicosapentaenoic acid and gamma-linolenic acid in ventilated patients with acute lung injury. Crit Care Med. 2006; 34:1033–1038. [PubMed: 16484911]
12. Freedman SD, et al. Association of cystic fibrosis with abnormalities in fatty acid metabolism. New England Journal of Medicine. 2004; 350:560–569. [PubMed: 14762183]
13. Serhan CN, et al. Resolvins: a family of bioactive products of omega-3 fatty acid transformation circuits initiated by aspirin treatment that counter proinflammation signals. J Exp Med. 2002; 196:1025–1037. [PubMed: 12391014]
14. Sun YP, et al. Resolvin D1 and its aspirin-triggered 17R epimer. Stereochemical assignments, anti-inflammatory properties, and enzymatic inactivation. J Biol Chem. 2007; 282:9323–9334. [PubMed: 17244615]
15. Fukunaga K, Kohli P, Bonnans C, Fredenburgh LE, Levy BD. Cyclooxygenase 2 plays a pivotal role in the resolution of acute lung injury. J Immunol. 2005; 174:5033–5039. [PubMed: 15814734]
16. O'Neal HR, et al. Prehospital Statin Use Is Associated with a Lower Incidence of Sepsis and ALI. Am J Respir Crit Care Med. 2009; 179:A1155.
17. Krishnamoorthy S, et al. Resolvin D1 binds human phagocytes with evidence for proresolving receptors. Proc Natl Acad Sci U S A. 2010; 107:1660–1665. [PubMed: 20080636]
18. Krishnamoorthy S, Recchiuti A, Chiang N, Fredman G, Serhan CN. Resolvin D1 Receptor Stereoselectivity and Regulation of Inflammation and Proresolving MicroRNAs. American Journal of Pathology. 2012
19. Zarbock A, Singbartl K, Ley K. Complete reversal of acid-induced acute lung injury by blocking of platelet-neutrophil aggregation. J Clin Invest. 2006; 116:3211–3219. [PubMed: 17143330]

20. Looney MR, et al. Platelet depletion and aspirin treatment protect mice in a two-event model of transfusion-related acute lung injury. J Clin Invest. 2009; 119:3450–3461. [PubMed: 19809160]
21. Bonnans C, Fukunaga K, Levy MA, Levy BD. Lipoxin A(4) regulates bronchial epithelial cell responses to acid injury. Am J Pathol. 2006; 168:1064–1072. [PubMed: 16565483]
22. Chiang N, et al. The lipoxin receptor ALX: potent ligand-specific and stereoselective actions in vivo. Pharmacol Rev. 2006; 58:463–487. [PubMed: 16968948]
23. Norling LV, Dalli J, Flower RJ, Serhan CN, Perretti M. Resolvin D1 limits PMN recruitment to inflammatory loci: receptor dependent actions. Arteriosclerosis, Thrombosis, and Vascular Biology. 2012 in press.
24. Claria J, Serhan CN. Aspirin triggers previously undescribed bioactive eicosanoids by human endothelial cell-leukocyte interactions. Proc Natl Acad Sci U S A. 1995; 92:9475–9479. [PubMed: 7568157]
25. Serhan CN, Chiang N, Van Dyke TE. Resolving inflammation: dual anti-inflammatory and pro-resolution lipid mediators. Nat Rev Immunol. 2008; 8:349–361. [PubMed: 18437155]
26. Bento AF, Claudino RF, Dutra RC, Marcon R, Calixto JB. Omega-3 fatty acid-derived mediators 17(R)-hydroxy docosahexaenoic acid, aspirin-triggered resolvin D1 and resolvin D2 prevent experimental colitis in mice. J Immunol. 2011; 187:1957–1969. Epub 2011 Jul 1951. [PubMed: 21724996]
27. Lima-Garcia JF, et al. The precursor of resolvin D series and aspirin-triggered resolvin D1 display anti-hyperalgesic properties in adjuvant-induced arthritis in rats. Br J Pharmacol. 2011; 164:278–293. 210.1111/j.1476–5381.2011.01345.x. [PubMed: 21418187]
28. Abraham E. Neutrophils and acute lung injury. Crit Care Med. 2003; 31:S195–199. [PubMed: 12682440]
29. Knight PR, Druskovich G, Tait AR, Johnson KJ. The role of neutrophils, oxidants, and proteases in the pathogenesis of acid pulmonary injury. Anesthesiology. 1992; 77:772–778. [PubMed: 1416175]
30. Folkesson HG, Matthay MA, Hebert CA, Broaddus VC. Acid aspiration-induced lung injury in rabbits is mediated by interleukin-8-dependent mechanisms. J Clin Invest. 1995; 96:107–116. [PubMed: 7615779]
31. Kasuga K, et al. Rapid appearance of resolvin precursors in inflammatory exudates: novel mechanisms in resolution. J Immunol. 2008; 181:8677–8687. [PubMed: 19050288]
32. Wang B, et al. Resolvin D1 protects mice from LPS-induced acute lung injury. Pulm Pharmacol Ther. 2011; 24:434–441. [PubMed: 21501693]
33. Dartt DA, et al. Conjunctival goblet cell secretion stimulated by leukotrienes is reduced by resolvins D1 and E1 to promote resolution of inflammation. J. 2011; 186:4455–4466. Epub 2011 Feb 4428.
34. Chiang N, et al. Infection regulates pro-resolving mediators that lower antibiotic requirements. Nature. 2012; 484:524–528. 510.1038/nature11042. [PubMed: 22538616]
35. Levy BD, Clish CB, Schmidt B, Gronert K, Serhan CN. Lipid mediator class switching during acute inflammation: signals in resolution. Nat Immunol. 2001; 2:612–619. [PubMed: 11429545]
36. Schwab JM, Chiang N, Arita M, Serhan CN. Resolvin E1 and protectin D1 activate inflammation-resolution programmes. Nature. 2007; 447:869–874. [PubMed: 17568749]
37. Frenette PS, et al. Platelet-endothelial interactions in inflamed mesenteric venules. Blood. 1998; 91:1318–1324. [PubMed: 9454762]
38. Zarbock A, Ley K. The role of platelets in acute lung injury (ALI). Front Biosci. 2009; 14:150–158. [PubMed: 19273059]
39. Fredman G, Van Dyke TE, Serhan CN. Resolvin E1 regulates adenosine diphosphate activation of human platelets. Arterioscler Thromb Vasc Biol. 2010; 30:2005–2013. Epub 2010 Aug 2011. [PubMed: 20702811]
40. Mayer K, et al. Acute lung injury is reduced in fat-1 mice endogenously synthesizing n-3 fatty acids. Am J Respir Crit Care Med. 2009; 179:474–483. Epub 2009 Jan 2008. [PubMed: 19136374]
41. Bilal S, et al. Fat-1 transgenic mice with elevated omega-3 fatty acids are protected from allergic airway responses. Biochimie Biophysica Acta. 2011; 1812:1164–1169.

42. Haworth O, Cernadas M, Yang R, Serhan CN, Levy BD. Resolvin E1 regulates interleukin 23, interferon-gamma and lipoxin A4 to promote the resolution of allergic airway inflammation. Nat Immunol. 2008; 9:873–879. [PubMed: 18568027]

43. Yang R, Chiang N, Oh SF, Serhan CN. Metabolomics-lipidomics of eicosanoids and docosanoids generated by phagocytes. Curr. 2011; Chapter(Unit 14.26)

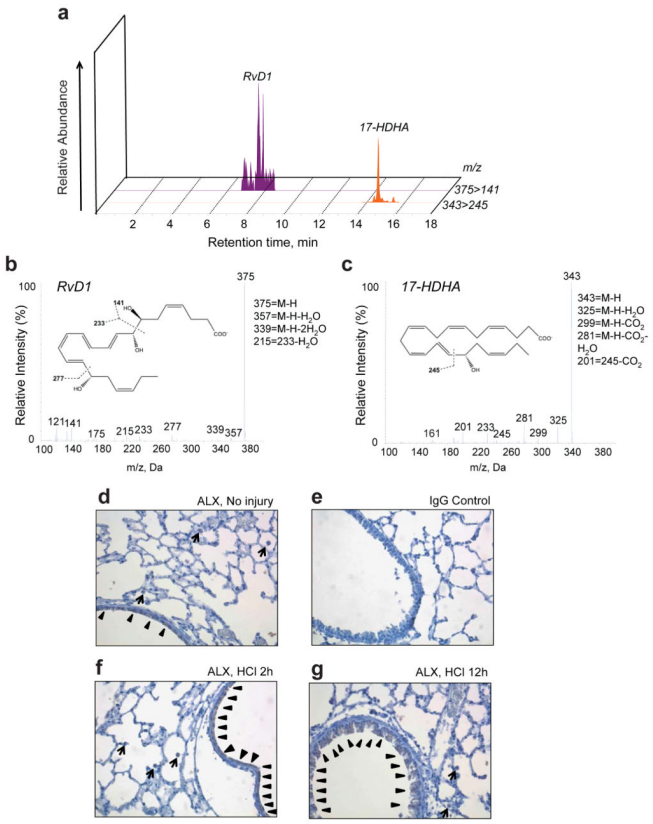

Figure 1. RvD1, 17-HDHA and ALX/FPR2 receptors are present in murine lungs after ALI

Murine lung homogenates were obtained 12hr after HCl-initiated ALI. Lipids were extracted and analyzed by LC-MS/MS. (**a**) MRM chromatograms (375>141 and 343>245) and representative tandem mass spectra of (**b**) RvD1 and (**c**) 17(S)-HDHA. Insets show structures and diagnostic fragmentation ions for each. Results are representative of n=3. Immunohistochemical analysis for ALX/FPR2 abundance was performed with lungs obtained (**d**) without injury exposed to ALX/FPR2 antibody (1/50) or (**e**) IgG control antibody, and (**f**) 2hr and (**g**) 12hr after ALI. Arrowheads, epithelial cells; Arrows, macrophages. Results are representative from n=3. Original magnification ×400

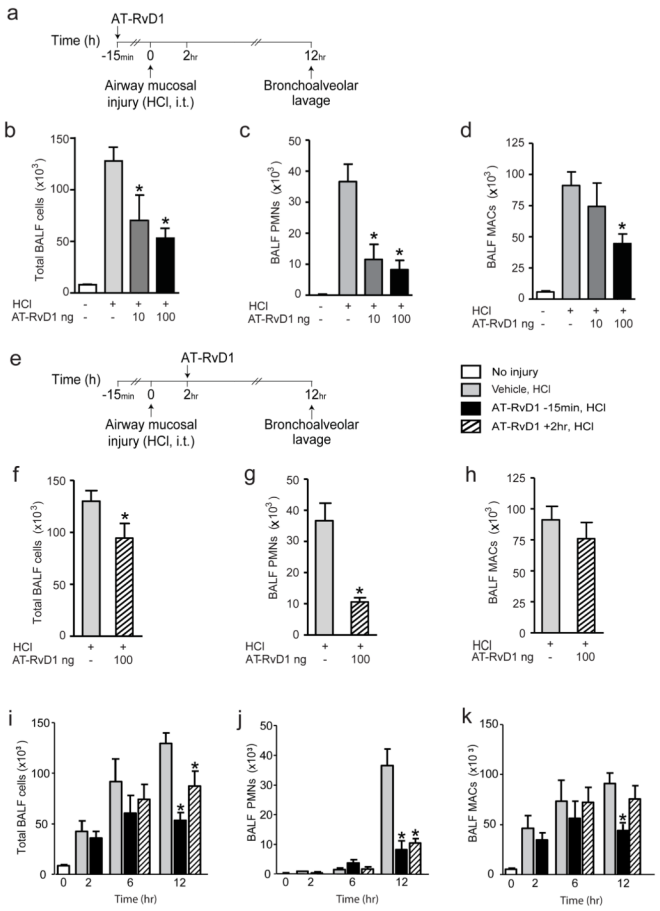

Figure 2. AT-RvD1 reduces leukocyte recruitment after airway mucosal injury

(**a**) AT-RvD1 (10ng, 100ng) or vehicle alone (0.1% ethanol in 0.9%NaCl (vol/vol)) were given intravenously 15 minutes prior to ALI. 12 hours later, BAL was performed and (**b**) total cells, (**c**) PMNs and (**d**) MACs in BALFs were enumerated (see Methods). (**e**) In a separate cohort, the impact of AT-RvD1 (100ng) or vehicle (0.1% ethanol in 0.9%NaCl (vol/vol)) given 2 hours after ALI was determined on BALF (**f**) total cells, (**g**) PMNs, and (**h**) MACs 12 hours after ALI was initiated. (**i–k**) Early leukocyte recruitment to the lung was assessed in the presence of AT-RvD1 (100ng, iv) or vehicle (0.1% ethanol in 0.9%NaCl (vol/vol)) given 15min before or 2hr after ALI. Values represent the mean ± SEM for n ≥ 5 mice. *, $p<0.05$ vs. vehicle group.

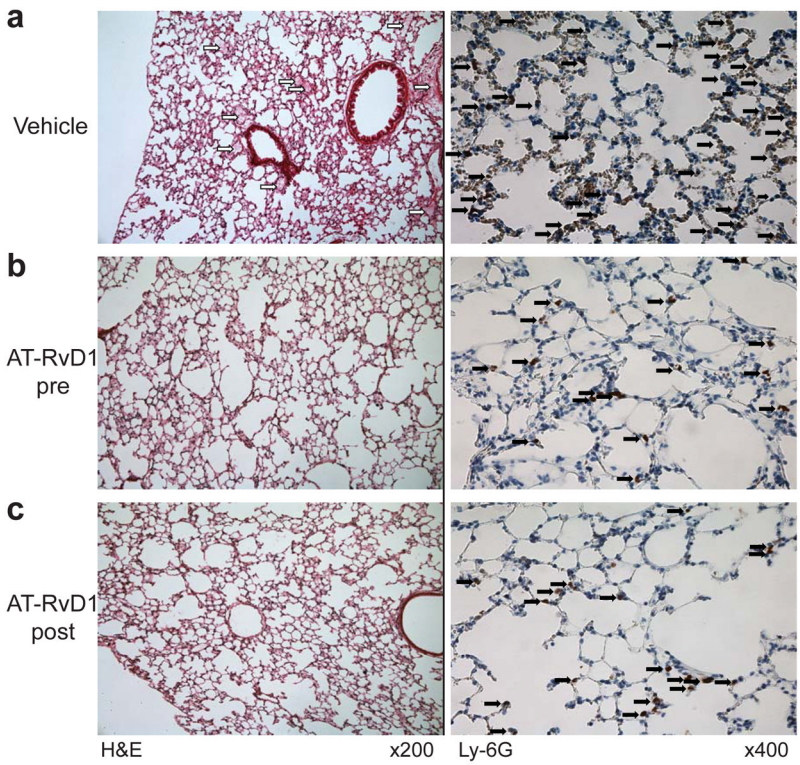

Figure 3. AT-RvD1 decreased the lung histopathologic changes after acid-initiated ALI

Lungs were obtained 12 hours after ALI from mice that were exposed to vehicle (0.1%ethanol in 0.9%NaCl (vol/vol), upper row (**a**)), AT-RvD1 (100ng) prior to ALI (middle row (**b**)) or AT-RvD1 (100ng) 2 hours after acid injury (lower row (**c**)). Lung tissue sections were prepared from fixed, paraffin embedded organs and stained with either hematoxylin and eosin (H&E) (left) or Ly-6G (1/100 dilution) (right) (see Methods). Alveolar edema (white arrows) and leukocytes (black arrows) are highlighted in representative images (n = 3); original magnification of H&E was x200 and Ly-6G was x400.

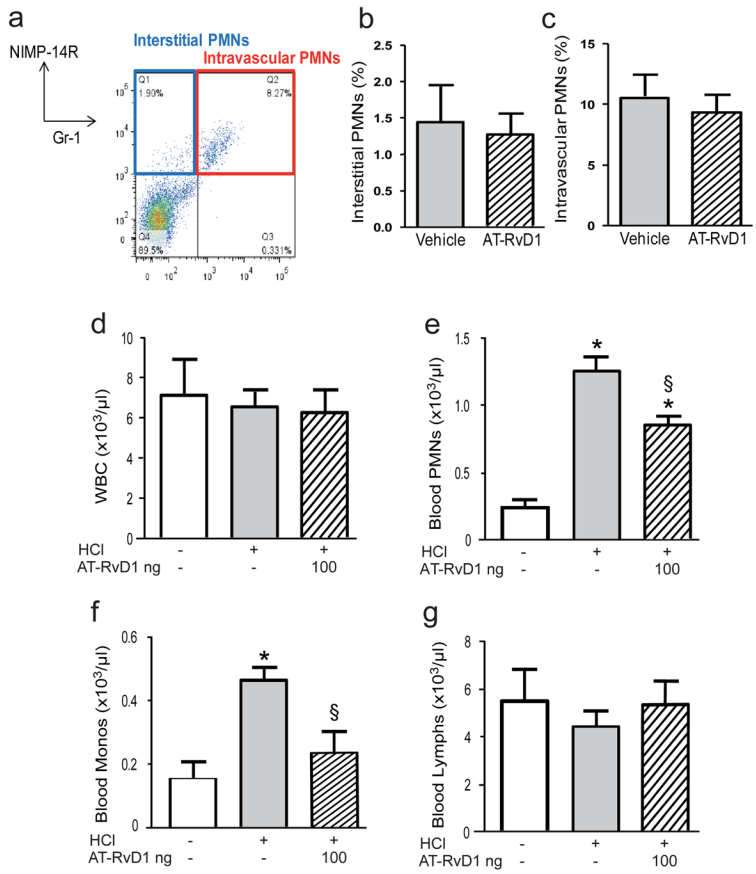

Figure 4. AT-RvD1 decreased peripheral blood leukocytosis to decrease lung recruitment after ALI

(**a**) Intravascular PMNs (NIMP-14R^{+}Gr-1^{+}) were distinguished from interstitial PMNs (NIMP-14R^{+}Gr-1^{-}) by FACS in (**b–c**) lungs obtained 12h after ALI from mice that were exposed to vehicle or AT-RvD1 (100ng) 2h after intratracheal acid instillation. Whole blood was collected 12h after ALI and (**d**) total leukocytes (WBC), (**e**) PMNs (**g**) monocytes (Monos) and (**h**) lymphocytes (Lymphs) were enumerated. Values represent the mean ± SEM for n ≥ 3 mice. *, $p<0.05$ vs. control group. §, $p<0.05$ vs. vehicle group.

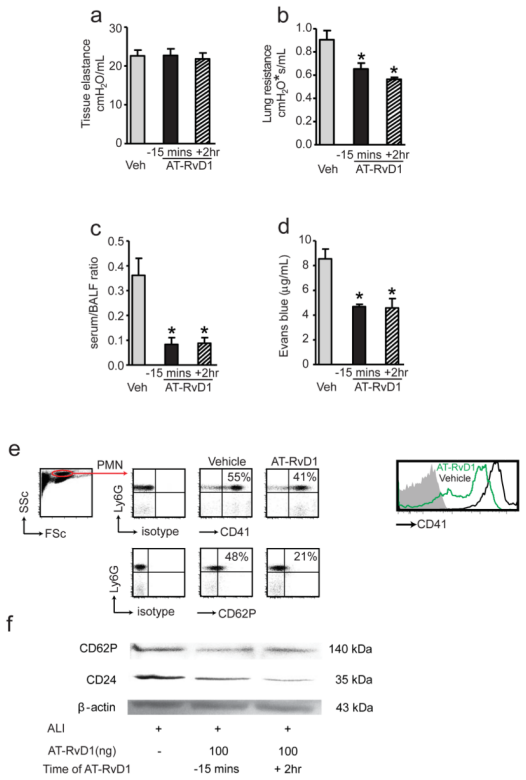

Figure 5. Counter-regulatory actions for AT-RvD1 on lung mechanics, barrier integrity and vascular inflammation after ALI

12h after ALI in mice exposed to AT-RvD1 (100 ng) or vehicle, lung mechanics were determined using a flexiVent mouse ventilator, including (**a**) tissue elastance and (**b**) lung resistance (see Methods). Values represent the mean ± SEM for n ≥ 6 mice. *, $p<0.05$ vs. vehicle group. (**c**) Epithelial and (**d**) endothelial barrier integrity 12h after ALI was determined in separate animals with intratracheal FITC-dextran and intravenous Evans blue dye, respectively (see Methods). Values represent the mean ± SEM for n ≥ 3 mice. *, $p<0.05$ vs. vehicle group. (**e**) Cell-cell interactions between PMNs and platelets were monitored by flow cytometry. Representative (n = 3) detection of $Ly6G^+CD41^+$ and $Ly6G^+CD62P^+$ cells in murine blood 12h after ALI. The percentages of positive cells are indicated at the top of the respective gates. (**f**) Representative (n ≥ 3) Western analysis for abundance in lung homogenates 12h after ALI of CD62P and CD24 (see Methods).

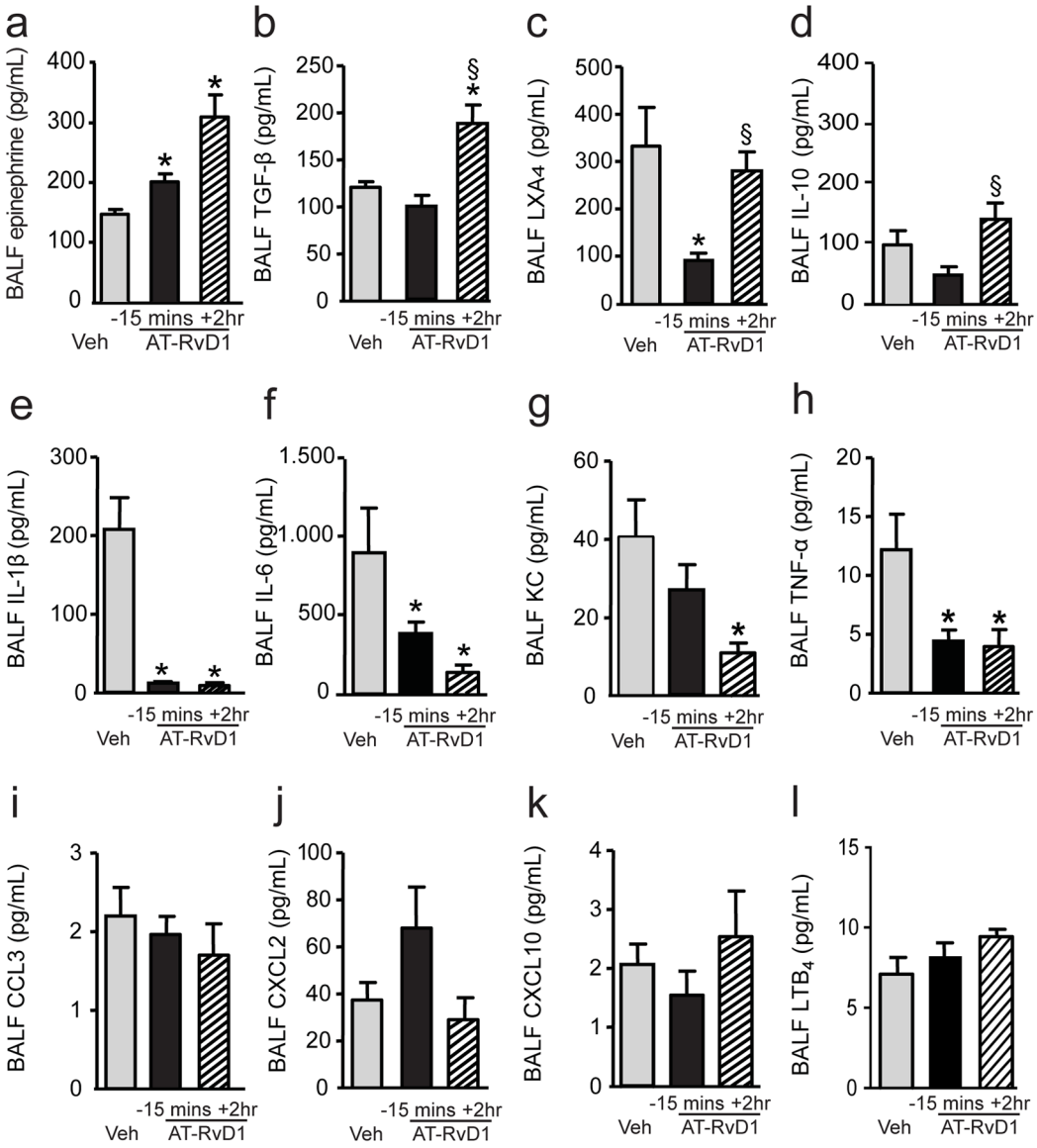

Figure 6. Impact of AT-RvD1 on inflammatory mediator levels after ALI

Aliquots of BALFs obtained 12h after ALI were analyzed by ELISA (**a,c,d,l**) or cytokine bead array (**b, e–k**). Values represent the mean ± SEM for n ≥ 3 mice. *, $P < 0.05$ vs. vehicle group. §, $P < 0.05$ vs 100ng AT-RvD1 group 15min before ALI.

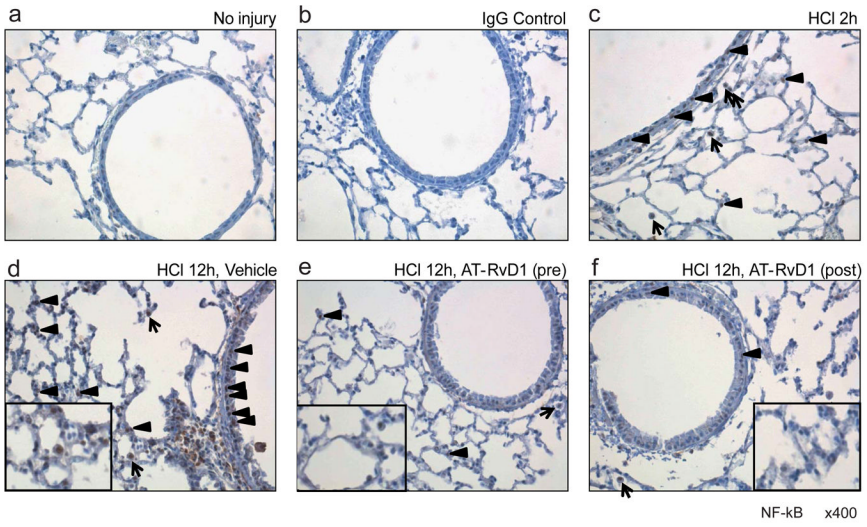

Figure 7. AT-RvD1 decreased ALI-induced NF-κB p65 activation and nuclear translocation in murine lung

Immunohistochemical analysis to detect NF-κB localization was performed by staining lung tissue (a) without injury using NF-κB phosphorylated p65 antibody (phospho S276, 1/50) or (b) IgG control antibody and (c) 2h after ALI. Lungs were also obtained 12h after ALI from mice exposed to (d) vehicle or (e,f) AT-RvD1 (100 ng). Insets, higher magnification to show nuclear staining. Arrowheads, epithelial cells; Arrows, macrophages. Results are representative from n=3. Original magnification ×400.